Spin-polarized quantum transport through a *T*-shape quantum dot-array: Model of spin splitter

Rui Wang and J.-Q. Liang*

Institute of Theoretical Physics, Shanxi University, Taiyuan 030006, China

(Received 3 February 2006; revised manuscript received 21 August 2006; published 5 October 2006)

We in this paper study theoretically the spin-polarized quantum transport through a *T*-shape quantum dot-array by means of transfer-matrix method along with the Green's function technique. Multimagnetic fields are used to produce the spin-polarized transmission probabilities and therefore the spin currents, which are shown to be tunable in a wide range by adjusting the energy, and the direction angle of magnetic fields as well. Particularly the opposite-spin-polarization currents separately flowing out to two electrodes can be generated and thus the system acts as a spin splitter.

DOI: 10.1103/PhysRevB.74.144302 PACS number(s): 72.25.−b, 73.23.−b, 73.21.La, 73.50.Bk

I. INTRODUCTION

Recent progress in the nanofabrication of quantum devices enables us to study electron transport through quantum dots (QDs) in a controllable way[1–3] since a wide range of energy can be achieved here by continuously changing the applied external potential in contrast with real atoms. A QD-array regarded as an artificial crystal[4–6] also becomes reliable due to the recent development of nanotechnology. When the size of the structures is small with respect to the coherence length, the transmission probability plays an essential role in the quantum transport. For example, we can obtain the conductance of the devices from the transmission probability with the help of the Laudauer-Büticker formula. Various methods have been developed for numerical calculations of the transmission probability.[7–18] The quantum transport through a multiterminal system[23–25] can be analyzed in terms of all transmission probabilities between any pair of terminals in principle. Büticker *et al.*[19] derived a scattering matrix for a three-terminal junction consisting of homogeneous wires based on the unitary condition and the assumption that the scattering matrix is real. It was shown that this matrix is energy independent and the coupling parameter has to be determined from phenomenological arguments.[20,21] An energy-dependent scattering matrix for the three-terminal junction was found later.[22]

Spintronics has become a new branch of condensed matter physics and material science where not only the charge but also the spin degree of freedom of electrons play an essential role.[26] It is of fundamental importance to study the mechanism to generate and control the spin-polarized currents in spintronic devices which may promise practical applications in quantum computing and information.[27,28] In recent years the spin-polarized transport in quantum dots has attracted considerable attention both theoretically[29–40] and experimentally,[41,42] where the spin currents are generated either by magnetic material electrodes or by the rotating-magnetic field which results in the spin flip. Most of the studies are concentrated on the one or two-QD devices with only one output electrode. The spin-polarized transport in QD-array consisting of an arbitrary number of QDs with multiterminal has not yet been investigated. In this paper we study the quantum transport through a *T*-shape QD-array with three electrodes in which the spin-polarized current is induced by static magnetic fields applied on the three arms of the *T*-shape QD-array. We calculate the transmission probability in terms of the scattering matrix which is spin-polarization dependent in the presence of magnetic fields and leads to the spin-polarized currents. It is the main goal of the present study to show how the spin currents in output terminals can be generated and controlled. Particularly two spin currents of opposite-spin-polarization flowing simultaneously out to electrodes are obtained and seem extremely useful in the design of quantum-logic-gate devices.

II. MODEL AND FORMULATION

The system consisting of three perfect wires (electrodes) attached to a *T*-shape QD-array of an arbitrary number of

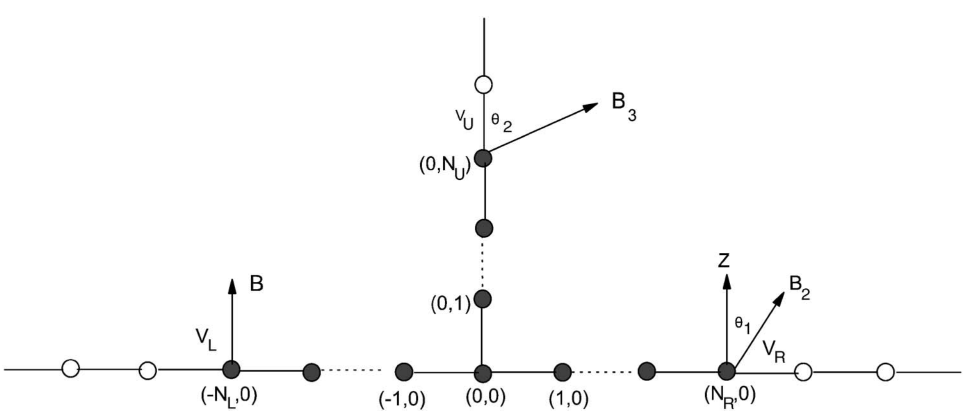

FIG. 1. *T*-shape QD-array of three electrode with three magnetic fields applied on the dots $(-N_L, 0)$, $(N_R, 0)$, and $(0, N_U)$, respectively.

QDs is explained schematically in Fig. 1. The horizontal QD-array is denoted by the lattice sites $(-N_L,0),(-N_L+1,0),\ldots,(0,0),\ldots,(N_R-1,0),(N_R,0)$ and the vertical QD-array by the lattice sites $(0,1),(0,2),\ldots,(0,N_U)$, where N_L, N_R, and N_U are the numbers of QDs on the left, right, and vertical arms, respectively. Three perfect wires are also described in terms of discrete lattice sites. The first magnetic field in the z direction is assumed to be applied, for example, on site $(-N_L,0)$, the second magnetic field on the site $(N_R,0)$ is along a direction of angle θ_1 with the z axis, while the third one on the site $(0,N_U)$ has a direction angle θ_2. The latter two magnetic fields not in the same direction as the first one result in the spin-flip of electrons, which is the mechanism generating the spin-polarized transport in the QD-array (see the Hamiltonian below). We remark that it is not necessary to have the three fields to apply on the certain single QD and what we choose the three QDs is only for the convenience of analysis. It may be easier in practical experiments to superpose the external fields on the three arms of the T-shape QD-array. The Hamiltonian of the system includes five parts

$$H = H_{d,h} + H_{d,v} + H_{el,h} + H_{el,v} + H_{d-el}, \tag{1}$$

where

$$\begin{aligned}
H_{d,h} = & \sum_{n=-N_L+1,\sigma}^{N_R-1} \varepsilon_{n,0} d^{+}_{(n,0),\sigma} d_{(n,0),\sigma} \\
& + (\varepsilon_{-N_L,0} + \sigma g \mu_B B) d^{+}_{(-N_L,0),\sigma} d_{(-N_L,0),\sigma} \\
& + (\varepsilon_{N_R,0} + \sigma g \mu_{B_1} B_1 \cos\theta_1) d^{+}_{(N_R,0),\sigma} d_{(N_R,0),\sigma} \\
& + g\mu_{B_1} B_1 \sin\theta_1 (d^{+}_{(N_R,0),\sigma} d_{(N_R,0),-\sigma} + \text{H.c.}) \\
& - \sum_{n=-N_L+1,\sigma}^{N_R-1} (t d^{+}_{(n+1,0),\sigma} d_{(n,0),\sigma} + \text{H.c.}) \\
& - (t' d^{+}_{(N_R-1,0),\sigma} d_{(N_R,0),\sigma} + \text{H.c.}) \\
& - (t' d^{+}_{(-N_L+1,0),\sigma} d_{(-N_L,0),\sigma} + \text{H.c.})
\end{aligned}$$

and

$$\begin{aligned}
H_{d,v} = & \sum_{n=0,\sigma}^{N_U-1} \varepsilon_{0,n} d^{+}_{(0,n),\sigma} d_{(0,n),\sigma} \\
& + (\varepsilon_{0,N_U} + \sigma g \mu_{B_2} B_2 \cos\theta_2) d^{+}_{(0,N_u),\sigma} d_{(0,N_u),\sigma} \\
& + g\mu_{B_2} B_2 \sin\theta_2 (d^{+}_{(0,N_u),\sigma} d_{(0,N_u),-\sigma} + \text{H.c.}) \\
& - \sum_{n=0,\sigma}^{N_U-1} (t d^{+}_{(0,n+1),\sigma} d_{(0,n),\sigma} + \text{H.c.}) \\
& - (t' d^{+}_{(0,N_U),\sigma} d_{(0,N_U-1),\sigma} + \text{H.c.})
\end{aligned}$$

denote the Hamiltonians of the horizontal and vertical QD-arrays, respectively with $\varepsilon_{n,0}$ and $\varepsilon_{0,n}$ being the energy eigenvalues of corresponding QDs. $d^{+}_{(n,0),\sigma}$ and $d^{+}_{(0,n),\sigma}$ (with $\sigma=\uparrow,\downarrow$) are the creation operators of the electrons with spin index σ on the QDs, where $-\sigma$ denotes the opposite spin polarization with respect to σ. The Zeeman terms induced by the external fields on the sites $(N_R,0)$, and $(0,N_U)$ result in the spin flip. It should be emphasized that the θ_1 and θ_2 dependent terms describing the spin-flip in the Hamiltonian are the key mechanism of the spin-polarized transport in our system. The matrix elements defined by $\langle n+1,0|H|n,0\rangle = \langle 0,n+1|H|0,n\rangle = t$ denote the hopping integrals between the nearest neighbors of QDs and are independent of spin polarization, except for $n=N_R$, $n=-N_L-1$, and $n=N_U$, where Zeeman energy induced by the external magnetic fields leads to the energy-level splitting and therefore the imbalance of tunnel couplings between spin-up and spin-down electrons. The hopping matrix elements in connection with the QDs $(N_R,0)$, $(-N_L,0)$, and $(0,N_U)$ are assumed to be $\langle N_R,0|H|N_R-1,0\rangle = \langle -N_L,0|H|-N_L+1,0\rangle = \langle 0,N_U|H|0,N_U-1\rangle = t'$. The Hamiltonians of horizontal and vertical electrodes are written as follows:

$$\begin{aligned}
H_{el,h} = & \sum_{n\leq-(N_L+1),\sigma} \varepsilon_L a^{+}_{(n,0),\sigma} a_{(n,0),\sigma} \\
& - \sum_{n\leq-(N_L+2),\sigma} (t a^{+}_{(n+1,0),\sigma} a_{(n,0),\sigma} + \text{H.c.}) \\
& + \sum_{n\geq N_R+1,\sigma} \varepsilon_R a^{+}_{(n,0),\sigma} a_{(n,0),\sigma} \\
& - \sum_{n\geq N_R+2,\sigma} (t a^{+}_{(n+1,0),\sigma} a_{(n,0),\sigma} + \text{H.c.}),
\end{aligned}$$

$$\begin{aligned}
H_{el,v} = & \sum_{n\geq N_U+1,\sigma} \varepsilon_U a^{+}_{(0,n),\sigma} a_{(0,n),\sigma} \\
& - \sum_{n\geq N_U+2,\sigma} (t a^{+}_{(0,n+1),\sigma} a_{(0,n),\sigma} + \text{H.c.}),
\end{aligned}$$

where ε_R, ε_L, and ε_U are the onsite energies in the right-hand side, the left-hand side, and the vertical electrodes, respectively. $a^{+}_{(n,0),\sigma}$ and $a^{+}_{(0,n),\sigma}$ are the creation operators of electrons in the electrodes. Finally the hopping of electrons between the QD and electrode is described by

$$\begin{aligned}
H_{d-el} = & - V_{L,\sigma}(a^{+}_{(-N_L-1,0),\sigma} d_{(-N_L,0),\sigma} + \text{H.c.}) \\
& - V_{R,\sigma}(a^{+}_{(N_R+1,0),\sigma} d_{(N_R,0),\sigma} + \text{H.c.}) \\
& - V_{U,\sigma}(a^{+}_{(0,N_U+1),\sigma} d_{(0,N_U),\sigma} + \text{H.c.}),
\end{aligned}$$

where $V_{R,\sigma}$, $V_{L,\sigma}$, $V_{U,\sigma}$, respectively denote the tunnel couplings between the three special QDs, where the magnetic fields are applied, and corresponding electrodes.

The main quantities which we have to calculate in our formulation are the transmission probabilities T_{ij} of electrons from electrode j to electrode i, and the reflection probabilities R_{jj} in the electrode j which is considered as an input terminal. For our three-terminal system we have $j=1$ (the left electrode) and $i=2,3$ (the right and vertical electrodes) with T_{21} denoting the transmission probability from the left to right electrodes and T_{31} from the left to vertical electrodes. However, the situation is not simple for the evaluation of transmission and reflection probabilities in the multiterminal system since the electron transport between two electrodes is by no means an isolated process but affected by other electrodes. To this end we begin with the stationary Shrödinger equation

$$H|\Psi\rangle = E|\Psi\rangle, \tag{2}$$

which possesses a general solution of the form

$$|\Psi\rangle = \sum_{n=-\infty,\sigma}^{\infty} C_{(n,0),\sigma} a^{+}_{(n,0),\sigma}|0\rangle + \sum_{n=1,\sigma}^{\infty} C_{(0,n),\sigma} a^{+}_{(0,n),\sigma}|0\rangle. \tag{3}$$

Inserting Eq. (3) into the Shrödinger equation (2) yields

$$\begin{aligned}
&(E-\varepsilon_{n,0})C_{(n,0),\sigma} + tC_{(n-1,0),\sigma} + tC_{(n+1,0),\sigma} = 0, n \neq -N_L, 0, N_R,\\
&(E-\varepsilon_{0,n})C_{(0,n),\sigma} + tC_{(0,n-1),\sigma} + tC_{(0,n+1),\sigma} = 0, n \neq N_U, (n \geqslant 1),\\
&(E-\varepsilon_{0,0})C_{(0,0),\sigma} + tC_{(0,1),\sigma} + tC_{(-1,0),\sigma} + tC_{(1,0),\sigma} = 0, n = 0,
\end{aligned} \tag{4}$$

$$(E-(\varepsilon_{-N_L,0}+\sigma g\mu_B B))C_{(-N_L,0),\sigma} + V_{L,\sigma}C_{-N_L-1,\sigma} + t' C_{-N_L+1,\sigma} = 0, \tag{5}$$

$$(E-(\varepsilon_{N_R,0}+\sigma g\mu_{B_1}B_1\cos\theta_1))C_{(N_R,0),\sigma} + B_1\sin\theta_1 C_{(N_R,0),-\sigma} + t' C_{(N_R-1,0),\sigma} + V_{R,\sigma}C_{(N_R+1,0),\sigma} = 0, \tag{6}$$

$$(E-(\varepsilon_{0,N_U}+\sigma g\mu_{B_2}B_2\cos\theta_2))C_{(0,N_U),\sigma} + B_2\sin\theta_2 C_{(0,N_U),-\sigma} + t' C_{(0,N_U-1),\sigma} + V_{U,\sigma}C_{(0,N_U+1),\sigma} = 0. \tag{7}$$

Notice that in the input electrode 1 the wave function is a superposition of the incoming plane wave of unit amplitude and a reflection wave with amplitude $r_{11}(\sigma)$, while in the output electrodes 2, 3 the outgoing plane waves possess transmission amplitudes $t_{21}(\sigma)$ and $t_{31}(\sigma)$, respectively, we have

$$C_{(n,0),\sigma} = e^{iK^L_\sigma na} + r_{11}(\sigma)e^{-iK^L_\sigma na}, \quad n \leqslant -(N_L+1), \tag{8}$$

$$C_{(n,0),\sigma} = t_{21}(\sigma)e^{iK^R_\sigma na}, \quad n \geqslant N_R+1, \tag{9}$$

$$C_{(0,n),\sigma} = t_{31}(\sigma)e^{iK^U_\sigma na}, \quad n \geqslant N_U+1, \tag{10}$$

where, K^L_σ, K^R_σ, and K^U_σ are the wave vectors in the left-, right-, and vertical-electrode, respectively. Using these wave functions, we can eliminate all the coefficients, $\{C_{(0,n),\sigma}\}$, in Eq. (4) and Eq. (7) and obtain

$$\begin{aligned}
&(E-\varepsilon_{n,0})C_{(n,0),\sigma} + tC_{(n-1,0),\sigma} + tC_{(n+1,0),\sigma} = 0, n \neq -N_L, 0, N_R,\\
&(E-(\varepsilon_{0,0}+\varepsilon^U_{0,0})\ C_{(0,0),\sigma} + tC_{(0,1),\sigma} + tC_{(-1,0),\sigma} + tC_{(1,0),\sigma} = 0, n = 0
\end{aligned} \tag{11}$$

$$(E-(\varepsilon_{-N_L,0}+\sigma g\mu_B B))C_{(-N_L,0),\sigma} + V_{L,\sigma}C_{-N_L-1,\sigma} + t' C_{-N_L+1,\sigma} = 0, \tag{12}$$

$$(E-(\varepsilon_{N_R,0}+\sigma g\mu_{B_1}B_1\cos\theta_1))C_{(N_R,0),\sigma} + B_1\sin\theta_1 C_{(N_R,0),-\sigma} + t' C_{(N_R-1,0),\sigma} + V_{R,\sigma}C_{(N_R+1,0),\sigma} = 0, \tag{13}$$

where $\varepsilon_{0,0}+\varepsilon^U_{0,0}$ is the effective energy on site (0,0) with

$$\varepsilon^U_{0,0} = \cfrac{V^2_{U,\sigma}}{E-\varepsilon_{0,1}-\cfrac{t^2}{E-\varepsilon_{0,2}-\cfrac{t^2}{\ddots\cfrac{(t')^2}{E-\varepsilon_{0,N_U}-\sum^U(E)}}}}. \tag{14}$$

Here $\Sigma^U(E)=V^2_{U,\sigma}G^U(E)$ denotes the self-energy due to the coupling with the horizontal QD-array, and $G^U(E)$ is the Green's function of the lattice site $(0,N_U)$ satisfying the recursive equation

$$G^U(E) = [E-\varepsilon_U - t^2G^U(E)]^{-1}, \tag{15}$$

the solution of which is seen to be

$$G^U(E) = \frac{1}{2t^2}\{(E-\varepsilon_U) - i[4t^2-(E-\varepsilon_U)^2]^{1/2}\}. \tag{16}$$

We can see that, Eqs. (11)–(13) does not include any of the expansion coefficients, $\{C_{(0,n),\sigma}\}$, associated with the vertical lattice site. Thus it implies that the three-terminal device reduces to an effective two-terminal system and the effect of the vertical QD-array appears as a self-energy $\Sigma^U(E)$ which has now been included in the effective onsite energy.

Now we rewrite Eq. (11)–(13) as a matrix equation

$$\begin{bmatrix} C_{(n+1,0),\sigma} \\ C_{(n,0),\sigma} \\ C_{(n+1,0),-\sigma} \\ C_{(n,0),-\sigma} \end{bmatrix} = M[(n,0),E]\begin{bmatrix} C_{(n,0),\sigma} \\ C_{(n-1,0),\sigma} \\ C_{(n,0),-\sigma} \\ C_{(n-1,0),-\sigma} \end{bmatrix},$$

where $M[(n,0),E]$ is called the transfer matrix which links the expansion coefficient vector $(C_{(n+1,0),\sigma},C_{(n,0),\sigma},C_{(n+1,0),-\sigma},C_{(n,0),-\sigma})^T$ to the vector $(C_{(n,0),\sigma},C_{(n-1,0),\sigma},C_{(n,0),-\sigma},C_{(n-1,0),-\sigma})^T$ and thus is defined by

$$M[(n,0),E]=\begin{bmatrix} -\dfrac{E-\varepsilon'_{n,0}}{t} & -1 & 0 & 0 \\ 1 & 0 & 0 & 0 \\ 0 & 0 & -\dfrac{E-\varepsilon'_{n,0}}{t} & -1 \\ 0 & 0 & 1 & 0 \end{bmatrix}=\begin{bmatrix} Q_1 & 0 \\ 0 & Q_2 \end{bmatrix}, \quad n\neq N_R,$$

$$M[(N_R,0),E]=\begin{bmatrix} -\dfrac{E-\varepsilon'_{N_R,0}}{V_{R,\sigma}} & -\dfrac{t'}{V_{R,\sigma}} & \dfrac{g\mu_{B_1}B_1\sin\theta_1}{V_{R,\sigma}} & 0 \\ 1 & 0 & 0 & 0 \\ \dfrac{g\mu_{B_1}B_1\sin\theta_1}{V_{R,\sigma}} & 0 & -\dfrac{E-\varepsilon'_{N_R,0}}{V_{R,\sigma}} & -\dfrac{t'}{V_{R,\sigma}} \\ 0 & 0 & 1 & 0 \end{bmatrix}, \quad (n=N_R), \tag{17}$$

where $\varepsilon'_{(n,0)}$ is the effective onsite energy given by

$$\varepsilon'_{n,0}=\varepsilon_{n,0}, \quad n\neq -N_L,0,N_R,$$

$$\varepsilon'_{-N_L,0}=\varepsilon_{-N_L,0}+\sigma g\mu_B B, \quad n=-N_L,$$

$$\varepsilon'_{0,0}=\varepsilon_{0,0}+\varepsilon^U_{0,0}, \quad n=0,$$

$$\varepsilon'_{N_R,0}=\varepsilon_{N_R,0}+\sigma g\mu_{B_1}B_1\cos\theta_1, \quad n=-N_R. \tag{18}$$

From Eqs. (8) and (9), it can be shown that the transmission amplitude $t_{21}(\sigma)$ is related to the incident coefficients via the equation

$$\begin{bmatrix} t_{21}(\sigma) \\ 0 \\ t_{21}(-\sigma) \\ 0 \end{bmatrix}=T(E)\begin{bmatrix} 1 \\ r_{11}(\sigma) \\ 1 \\ r_{11}(-\sigma) \end{bmatrix}, \tag{19}$$

where the transfer matrix $T(E)$ for the whole system is given by

$$T(E)=\begin{bmatrix} e^{-iK^R_\sigma(N_R+1)a} & 0 & 0 & 0 \\ 0 & e^{iK^R_\sigma(N_R+1)a} & 0 & 0 \\ 0 & 0 & e^{-iK^R_{-\sigma}(N_R+1)a} & 0 \\ 0 & 0 & 0 & e^{iK^R_{-\sigma}(N_R+1)a} \end{bmatrix}\times\begin{bmatrix} e^{ik^R_\sigma a} & e^{-ik^R_\sigma a} & 0 & 0 \\ 1 & 1 & 0 & 0 \\ 0 & 0 & e^{ik^R_{-\sigma}a} & e^{-ik^R_{-\sigma}a} \\ 0 & 0 & 1 & 1 \end{bmatrix}^{-1}\prod_{n=N_R+1}^{-(N_L+1)} M[(n,0),E]$$
$$\times\begin{bmatrix} e^{ik^L_\sigma a} & e^{-ik^L_\sigma a} & 0 & 0 \\ 1 & 1 & 0 & 0 \\ 0 & 0 & e^{ik^L_{-\sigma}a} & e^{-ik^L_{-\sigma}a} \\ 0 & 0 & 1 & 1 \end{bmatrix}\begin{bmatrix} e^{-iK^L_\sigma(N_L+1)a} & 0 & 0 & 0 \\ 0 & e^{iK^L_\sigma(N_L+1)a} & 0 & 0 \\ 0 & 0 & e^{-iK^L_{-\sigma}(N_L+1)a} & 0 \\ 0 & 0 & 0 & e^{iK^L_{-\sigma}(N_L+1)a} \end{bmatrix}. \tag{20}$$

Thus from Eq. (19) we can obtain the reflection amplitudes $r_{11}(\uparrow)$ and $r_{11}(\downarrow)$ as follows:

$$r_{11}(\uparrow)=\frac{-\left(\frac{T_{21}}{T_{22}}+\frac{T_{23}}{T_{22}}\right)+\frac{T_{24}}{T_{22}}\left(\frac{T_{41}}{T_{44}}+\frac{T_{43}}{T_{44}}\right)}{1-\frac{T_{24}}{T_{22}}\frac{T_{42}}{T_{44}}}, \tag{21}$$

$$r_{11}(\downarrow)=\frac{-\left(\frac{T_{41}}{T_{44}}+\frac{T_{43}}{T_{44}}\right)+\frac{T_{42}}{T_{44}}\left(\frac{T_{21}}{T_{22}}+\frac{T_{23}}{T_{22}}\right)}{1-\frac{T_{24}}{T_{22}}\frac{T_{42}}{T_{44}}}, \tag{22}$$

and the transmission amplitudes $t_{21}(\uparrow)$ and $t_{21}(\downarrow)$,

$$t_{21}(\uparrow)=T_{11}+T_{12}r_{11}(\uparrow)+T_{13}+T_{14}r_{11}(\downarrow), \tag{23}$$

$$t_{21}(\downarrow)=T_{31}+T_{32}r_{11}(\uparrow)+T_{33}+T_{34}r_{11}(\downarrow). \tag{24}$$

The spin-polarized reflection and transmission probabilities are seen to be

$$R_{11}(\sigma)=\frac{1}{2}|r_{11}(\sigma)|^2, \tag{25}$$

$$T_{21}(\sigma)=\frac{1}{2}\frac{V_{R,\sigma}}{V_{L,\sigma}}|t_{21}(\sigma)|^2, \tag{26}$$

and the total transmission and reflection probabilities are defined by

$$T_{21,tot}=T_{21}(\uparrow)+T_{21}(\downarrow), \tag{27}$$

$$R_{11,tot}=R_{21}(\uparrow)+R_{21}(\downarrow). \tag{28}$$

The spin current can be derived from the difference between the two spin-polarized transmission probabilities

$$\Delta T_{21}=T_{21}(\uparrow)-T_{21}(\downarrow). \tag{29}$$

The transmission probability, $T_{31}(\sigma)$, from electrode 1 to electrode 3 can be simply obtained by replacing the onsite energy $\varepsilon'_{0,0}=\varepsilon_{0,0}+\varepsilon^U_{0,0}$ in the matrix $M[(0,0),E]$ with $\varepsilon'_{0,0}=\varepsilon_{0,0}+\varepsilon^R_{0,0}$, where

$$\varepsilon^R_{0,0}=\cfrac{V^2_{R,\sigma}}{E-\varepsilon_{1,0}-\cfrac{t^2}{E-\varepsilon_{2,0}-\cfrac{t^2}{\ddots\,\cfrac{(t')^2}{E-\varepsilon_{N_R,0}-\sum^R(E)}}}}, \tag{30}$$

and $\Sigma^R(E)=V^2_{R,\sigma}G^R(E)$ is the self-energy due to the presence of the right electrode, and

$$G^R(E)=[E-\varepsilon_U-t^2G^R(E)]^{-1}, \tag{31}$$

is the Green's function of the lattice-site $(N_R+1,0)$. Moreover the effective onsite energy $\varepsilon'_{n,0}$ of Eq. (18) should be replaced by

$$\varepsilon'_{0,n}=\varepsilon_{0,n},\quad n\neq -N_L,0,N_U,$$

$$\varepsilon'_{-N_L,0}=\varepsilon_{-N_L,0}+\sigma g\mu_B B,\quad n=-N_L,$$

$$\varepsilon'_{0,0}=\varepsilon_{0,0}+\varepsilon^R_{0,0},\quad n=0,$$

$$\varepsilon'_{0,N_U}=\varepsilon_{0,N_U}+\sigma g\mu_{B_2}B_2\cos\theta_2,\quad n=N_U.$$

Then the transmission probability $T_{31}(\sigma)$ can be evaluated from

$$T_{31}(\sigma)=\frac{1}{2}\frac{V_{U,\sigma}}{V_{L,\sigma}}|t_{31}(\sigma)|^2, \tag{32}$$

and finally we obtain the total and spin transmission probabilities $T_{31,tot}$, ΔT_{31} in the same way as for the calculation of $T_{21,tot}$ and ΔT_{21}.

The conductance of the device can be obtained from the transmission probability with the help of the Laudauer-Büticker formula

$$G=\left(\frac{2e^2}{h}\right)T, \tag{33}$$

where e is the electron charge, h the Planck's constant, and T the transmission probability of the device.

III. NUMERICAL RESULT AND DISCUSSION

A. Homogeneous dot array

In the numerical evaluation the lattice constant a is chosen as a unit of length and the hopping constant t as the unit of energy. The onsite energies of all QDs, as well as ε_L, ε_R, ε_U are set to the same value of $2t$. The coupling parameters between the QDs and the three electrodes are assumed to be $V_{L,\sigma}=V_{R,\sigma}=V_{U,\sigma}=0.5t$, and $g\mu_{B_1}B_1=g\mu_{B_2}B_2=1t$.

First of all we consider the simplest case that there is only one QD on each arm of the T-shape array besides the central dot, i.e., $N_L=N_R=N_U=1$. Figures 2(a), 3(a), 2(b), and 3(b) display the energy dependence (spectrum) of the spin-up and the spin-down transmission probabilities to the electrode-2 and the electrode-3, respectively (for $t=1$, $t'=0.8$, $\theta_1=\frac{3}{4}\pi$, $\theta_2=\frac{1}{4}\pi$). The total transmissions $T_{21,tot}$, $T_{31,tot}$ are shown in Figs. 4(a) and 4(b). It can be seen that in the presence of the external magnetic fields, the transmitted electrons split into spin-up and spin-down components with different spectra. Figure 5 is the plot of the relative transmission probabilities between two spin components ΔT_{21} (solid line) and ΔT_{31} (dotted line) versus the energy, respectively. We can see that in some electron-energy ranges, for example from $1.8t$ to $2.4t$ or from $3.4t$ to $3.8t$, the spin transmission probability to the electrode 3, ΔT_{31}, is positive (i.e., the spin current with spin-up polarization) while the spin transmission probability

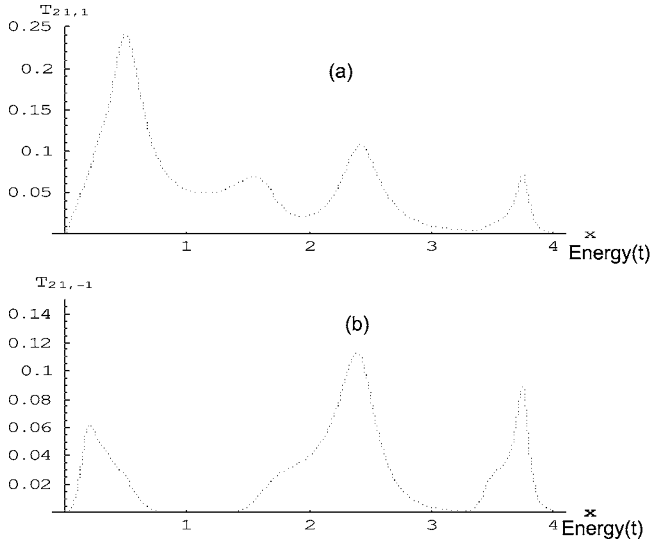

FIG. 2. Spin-up (a) and spin-down transmission probabilities to the electrode-2 as a function of energy.

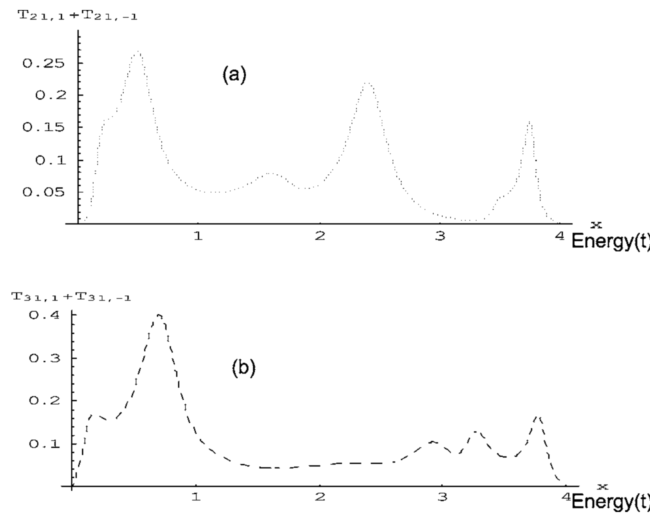

FIG. 4. Total transmission probabilities to electrode-2 and electrode-3.

to electrode 2, ΔT_{21}, is negative (namely the spin-down current). However, the situation would be opposite in other energy region, for example from $0t$ to $1.2t$, where ΔT_{21} is positive and ΔT_{31} is negative.

Figure 6 shows the spin transition probabilities ΔT_{21} (solid line) and ΔT_{31} (dotted line) as a function of energy for the multi-QD case that $N_L = N_R = 4$ and $N_U = 3$ with the magnetic field direction angles $\theta_1 = \theta_2 = \frac{1}{2}\pi$. In the electron-energy range from $0.6t$ to $0.75t$ or from $1.78t$ to $1.90t$ the spin transmission probability ΔT_{31} is positive (i.e., the spin-up current flowing to electrode 3) while ΔT_{21} is negative (spin-down current flowing to electrode 2). Opposite spin currents are observed in the energy region from $0.38t$ to $0.47t$, where ΔT_{31} is positive and ΔT_{21} is negative. Figure 7 is the result of ΔT_{21} (solid line) and ΔT_{31} (dotted line) for the direction angles $\theta_1 = \frac{3}{4}\pi$ while $\theta_2 = \frac{1}{4}\pi$. We see that the spin currents are sensitive to the fields. It may also be worth pointing out that in the energy region between $2.9t$ and $3.1t$, ΔT_{21} is negligibly small while ΔT_{31} is positive. In other words the spin current can exist only in one output electrode. Comparing with previous case (one QD on each arm) more resonant peaks of the spectra appear with the increasing number of QDs in the same way as the usual quantum transport in the QD-array without spin polarization.

The generation of spin currents in the two output electrodes in our model can be understood that a force applied on the spin **S** which is induced by the spatially inhomogeneous magnetic fields, namely $\mathbf{F} = g\mu_b \mathbf{S} \cdot \nabla \mathbf{B}$ (where μ_b is the Bohr magneton, g is the spin g factor), removes the degeneracy of spin polarization in the transport and thus leads to the relative shifts of resonant peaks of the transmission spectra between the spin-up and spin-down components of the electron. The spin current appears when the transmission spectrum of one spin component reaches a maximum while the spectrum of the other spin component is a minimum.

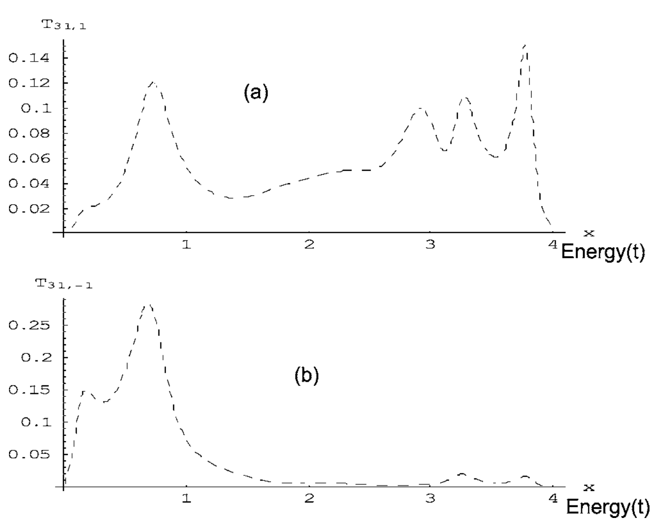

FIG. 3. Spin-up (a) and spin-down transmission probabilities to the electrode-3 as a function of energy.

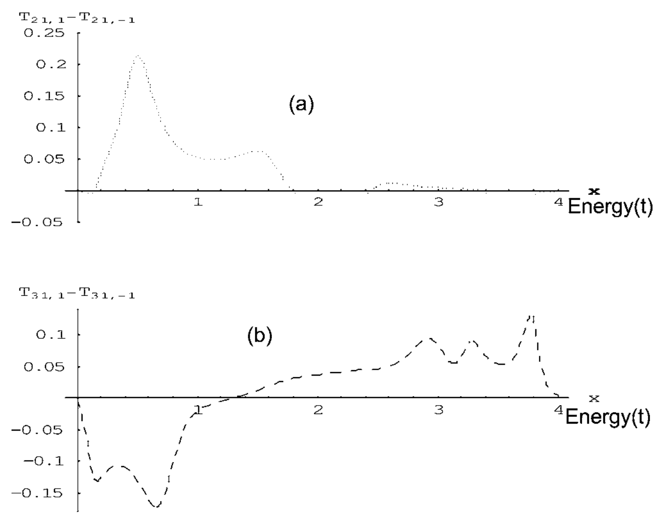

FIG. 5. Spin-polarized transmission probabilities to electrode-2 and electrode-3.

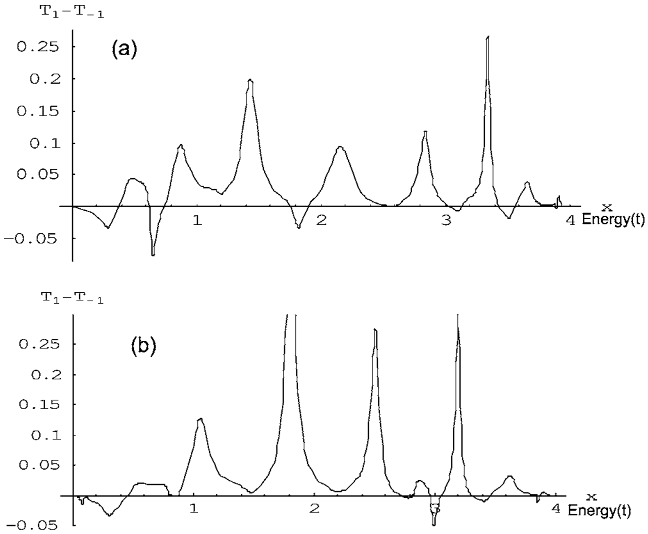

FIG. 6. Spin-polarized transmission probabilities to electrode-2 (solid line) and electrode-3 (dotted line) versus the energy for angles $\theta_1 = \frac{1}{2}\pi$ and $\theta_2 = \frac{1}{2}\pi$.

B. Effect of disorder

The homogeneous dot array is just a theoretical idealization and disorder is necessary to be taken into account in practical systems. It is interesting to see the disorder effect of the QD-array on the spin-polarized quantum transport. To this end we consider the disorder following Refs. 43–47 that the onsite energies of QDs are alternated with $4(1-x)$ and $4\cdot x$, where $0 \leqslant x \leqslant 1$ is the probability distribution parameter. When $x=0.5$, the system reduces to the nondisordering one. In the T-shape QD-array onsite energies $\varepsilon_{n,0}$ $(-N_L \leqslant n \leqslant N_R$, on the horizontal arm) and $\varepsilon_{0,n}$ $(1 \leqslant n \leqslant N_U$, on the vertical arm) are set to $4(1-x)$ for odd n and $4x$ for even n. Figure 8 is a comparison of plots of ΔT_{31} for the probability distribution parameter $x=0.47$ (dotted line), 0.5 (solid line), respectively with $N_L = N_R = 4$ and $N_U = 3$. We can see that the disorder can shift the resonant peaks of the transmission probability ΔT_{31} slightly, and suppress the height of some peaks but no more then 20% while increase the height of other peaks no more than 18%. In other words the spin splitting is robust against the disorder.

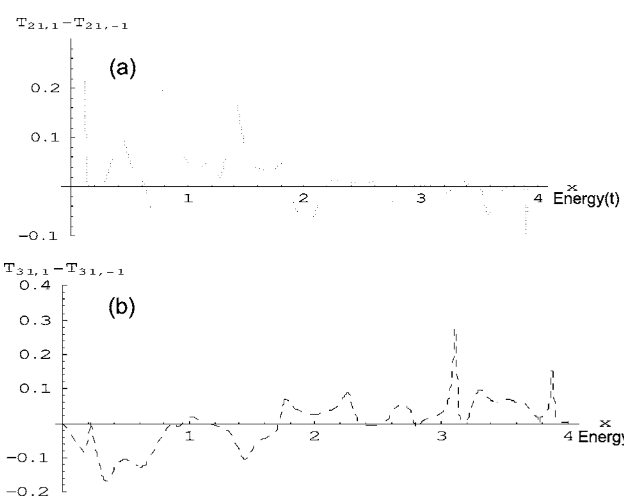

FIG. 7. Spin-polarized transmission probabilities to electrode-2 (solid line) and electrode-3 (dotted line) versus the energy for angles $\theta_1 = \frac{3}{4}\pi$ and $\theta_2 = \frac{1}{4}\pi$.

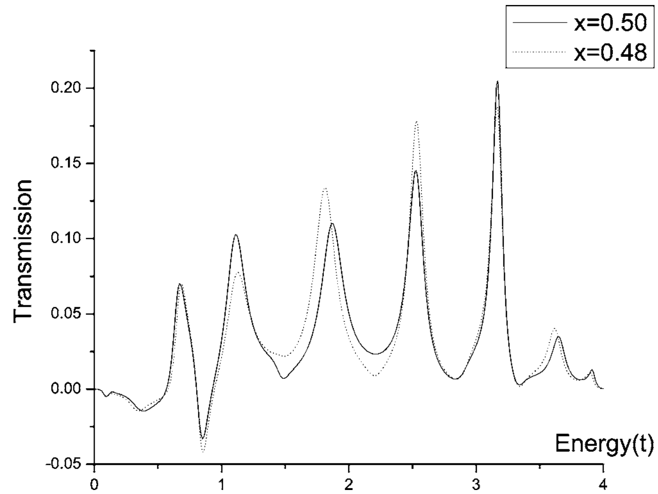

FIG. 8. The comparision of the plots ΔT_{31} with (dotted line) and without (solid line) the disoder for angles $\theta_1 = \frac{1}{2}\pi$ and $\theta_2 = \frac{1}{2}\pi$.

The latest advances in nanotechnology make it possible to fabricate QD-array[3] and the model of spin splitter proposed in this paper may be realizable experimentally. In a practical experiment it is more easy to apply the external fields on three arms of the T-shape QD-array instead of three QDs. The relative shifts of resonant peaks of the transmission spectra between the spin-up and spin-down components of electron can be modulated by the magnetic fields and onsite energies.

IV. SUMMARY AND CONCLUSION

In this paper we demonstrate theoretically a method to generate and control spin currents in a three-terminal system. The output spin currents are tunable in a wide range of magnitudes and various output configurations by adjusting the energy and the direction angles of the magnetic fields as well. Moreover it is demonstrated by the numerical evaluation that the spin currents remain in the presence of the disorder of QD-array. Particularly the spin currents with opposite spin polarizations in the two output electrodes can be generated. Thus this device is, as a matter of fact, a spin splitter similar to the light beam polarimeter in optics. This observation may have practical application in the fabrication of spintronic devices for logic gates with spin-up and spin-down outputs regarding qubits.

ACKNOWLEDGMENT

This work was supported by National Natural Science Foundation of China under Grant No. 10475053.

*Email address: jqliang@sxu.edu.cn

[1] D. Goldnaber-Gordon, H. Shtrikman, D. Mahalu, D. Abusch-Magder, U. Meirav, and M. A. Kastner, Nature (London) **391**, 156 (1998).
[2] S. M. Cronenwett, T. H. Oosterkamp, and L. P. Kouwenhoven, Science **281**, 540 (1998).
[3] P. A. Orellana, F. Dominguez-Adame, I. Gomez, and M. L. Ladron de Guevara, Phys. Rev. B **67**, 085321 (2003).
[4] A. W. Holleitner, C. R. Dedcker, H. Qin, K. Ebert, and R. H. Blick, Phys. Rev. Lett. **87**, 256802 (2001).
[5] A. W. Holleitner, R. H. Blick, A. K. Huttel, K. Ebert, and J. P. Kottaus, Science **297**, 70 (2002).
[6] W. Z. Shangguan, T. C. Au Yeung, Y. B. Yu, and C. H. Kam, Phys. Rev. B **63**, 235323 (2001).
[7] G. Kirczenow, Phys. Rev. B **39**, 10452 (1989).
[8] S. E. Ulloa, E. Castaňo, and G. Kirczenow, Phys. Rev. B **41**, 12350 (1990).
[9] J. A. Brum, Phys. Rev. B **43**, 12082 (1991).
[10] H. Tamura and T. Ando, Phys. Rev. B **44**, 1792 (1991).
[11] H. Wu, D. W. L. Sprung, J. Martorell, and S. Klarsfeld, Phys. Rev. B **44**, 6351 (1991).
[12] D. J. Thouless and S. Kirkpatrick, J. Phys. C **14**, 235 (1981).
[13] P. A. Lee and D. S. Fisher, Phys. Rev. Lett. **47**, 882 (1981).
[14] L. Schweizer, B. Kramer, and A. Mackinnon, J. Phys. C **17**, 4111 (1984).
[15] L. Schweizer, B. Kramer, and A. Mackinnon, Z. Phys. B: Condens. Matter **59**, 379 (1985).
[16] A. Mackinnon, Z. Phys. B: Condens. Matter **59**, 385 (1985).
[17] T. Ando, Phys. Rev. B **44**, 8017 (1991).
[18] H. Q. Xu, Phys. Rev. B **66**, 165305 (2002).
[19] M. Bütticker, Y. Imry, and M. Ya. Azbel, Phys. Rev. A **30**, 1982 (1984).
[20] P. A. Mello, Phys. Rev. B **47**, 16358 (1993).
[21] D. Takai and K. Ohta, Phys. Rev. B **48**, 1537 (1993).
[22] T. Itoh, Phys. Rev. B **52**, 1508 (1995).
[23] G. Bignon, M. Houzet, F. Pistlesi, and F. W. J. Hekking, Europhys. Lett. **67**(1), 110 (2004).
[24] T. B. Tran, I. Beloborodov, X. M. Lin, T. P. Bigioni, V. M. Vinokur, and H. M. Jaeger, Phys. Rev. Lett. **95**, 076806 (2005).
[25] C. Texier and G. Montambaux, Phys. Rev. Lett. **92**, 186801 (2004).
[26] Žutiéabian and S. Das Sarma, Rev. Mod. Phys. **76**, 323 (2004).
[27] S. A. Wolf *et al.*, Science **294**, 1488 (2001).
[28] G. A. Prinz, Science **282**, 1660 (1998).
[29] Y. Meir and N. S. Wingreen, Phys. Rev. Lett. **68**, 2512 (1992).
[30] A. Brataas, Y. Tserkovnyak, G. E. W. Bauer, and B. I. Halperin, Phys. Rev. B **66**, 060404(R) (2002).
[31] P. Sharma and C. Chamon, Phys. Rev. Lett. **87**, 096401 (2001); E. R. Mucciolo, C. Chamon, and C. M. Marcus, *ibid.* **89**, 146802 (2002).
[32] Q.-F. Sun, H. Guo, and J. Wang, Phys. Rev. Lett. **90**, 258301 (2003); J. Wu, B. Wang, and J. Wang, Phys. Rev. B **66**, 205327 (2002).
[33] B. Wang, J. Wang, and H. Guo, Phys. Rev. B **67**, 092408 (2003).
[34] T. Aono, Phys. Rev. B **67**, 155303 (2003).
[35] C. Benjamin and R. Citrol, cond-mat/0502589 (unpublished).
[36] K. Brkjel and A. Sudb, cond-mat/0506024 (unpublished).
[37] Qing-Feng Sun and X. C. Xie, cond-mat/0505517 (unpublished).
[38] Hui Yu and J.-Q. Liang, Phys. Rev. B **72**, 075351 (2005).
[39] B. Dong, H. L. Cui, S. Y. Liu, and X. L. Lei, J. Phys.: Condens. Matter **15**, 8435 (2003).
[40] B. Dong, H. L. Cui, and X. L. Lei, Phys. Rev. Lett. **94**, 066601 (2005).
[41] S. K. Watson, R. M. Potok, C. M. Marcus, and V. Umansky, Phys. Rev. Lett. **91**, 258301 (2003).
[42] M. J. Stevens, A. L. Smirl, R. D. R. Bhat, A. Najmaie, J. E. Sipe, and H. M. Van Driel, Phys. Rev. Lett. **90**, 136603 (2003); J. Hübner, W. W. Ruhle, M. Klude, D. Hommel, R. D. R. Bhat, J. E. Sipe, and H. M. Van Driel, Phys. Rev. Lett. **90**, 216601 (2003).
[43] M. Terraneo and I. Guarneri, Eur. Phys. J. B **B18**, 303 (2000).
[44] C. Texier and A. Comtet, Phys. Rev. Lett. **82**, 4220 (1999).
[45] F. A. Pinheiro, M. Rusek, A. Orlowski, and B. A. van Tiggelen, Phys. Rev. E **69**, 026605 (2004).
[46] M. Titov and Y. V. Fyodorov, Phys. Rev. B **61**, R2444 (2000).
[47] M. Weiss, J. A. Mendez-Bermudez, and T. Kottos, Phys. Rev. B **73**, 045103 (2006).